

# Dissipation-Reliability Tradeoff for Stochastic CMOS Bits in Series

Cathryn Murphy,<sup>1</sup> Schuyler Nicholson,<sup>1</sup> Nahuel Freitas,<sup>2,3</sup> Emanuele Penocchio,<sup>1,\*</sup> and Todd Gingrich<sup>1,†</sup>

<sup>1</sup>*Department of Chemistry, Northwestern University,  
2145 Sheridan Road, Evanston, Illinois 60208, USA*

<sup>2</sup>*Extropic Corporation, Cambridge, Massachusetts, USA*

<sup>3</sup>*Departamento de Física, FCEyN, UBA, Pabellón 1,  
Ciudad Universitaria, 1428 Buenos Aires, Argentina*

(Dated: March 6, 2026)

Physical instantiations of a bit of information are subject to thermal noise that can trigger unintended bit-flip errors. Bits implemented with CMOS technology typically operate in regimes that reliably suppress these errors with a large bias voltage, but miniaturization and circuit design for implantable biomedical devices motivate error suppression via alternative low-voltage strategies. We present and analyze an error-suppression technique that involves coupling multiple CMOS units into chains, introducing a natural error correction arising from inter-unit correlations. Using tensor networks to numerically solve a stochastic master equation for the CMOS chain, we quantify the reliability-dissipation tradeoff across system sizes that would be intractable with conventional sparse-matrix methods. The calculations show that the typical time for bit-flip errors scales exponentially with the bias voltage but subexponentially with the chain length. While a CMOS chain adds stability compared to a single CMOS unit for a fixed low bias voltage, increasing the bias voltage is a lower-dissipation route to equivalent stability.

*Introduction.* Classical computers rely on robust maintenance of logical bits, and any physical instantiation of those bits is subject to thermal noise [1]. That noise can stochastically trigger unintended bit-flip errors [2, 3], and it is important to be able to suppress the errors. A common strategy is implemented in CMOS devices, which involve complementary transistors powered by a supply voltage. When the supply increases, errors decrease, but at the expense of dissipating more energy. Engineering high-accuracy and low-dissipation devices has been a theoretical and practical goal for many decades [4–10].

Miniaturization and circuit design for implantable biomedical devices [11–13] both require low-power computing strategies, so we consider the dissipation-reliability balance when the supply voltage cannot simply be increased. The limitation on the supply voltage motivates us to consider an alternative way to mitigate errors: by building multiple error-prone CMOS units into a larger bistable system that encodes a single logical bit. We show that as the number of units in series increases, the bit grows more stable. Correlations between the units introduce a natural error correction that slows the rate of stochastic bit flips. The stability benefit is countered by the increased thermodynamic cost; each unit dissipates energy. While linear scaling of dissipation is easy to justify in terms of contributions from each unit, those units are strongly interacting. Errors require a rare event in one unit to trigger rare events in the others so the entire circuit can flip in a coordinated manner.

To demonstrate how that correlation effect emerges from essential physics, we build up to the collective dynamics by starting with a model that explicitly resolves

the dynamics and thermodynamics at the single electron level. Each electron hop triggers a transition to a new discrete state of the circuit. One can conceptually picture the circuit as if its state were confined to one basin of a double-well potential, occasionally flying over a barrier due to some Gaussian noise from the environment. That picture captures the essential bistability, but fails to provide a thermodynamically consistent connection between the energetics of the circuit and the thermal fluctuations [14–18]. Previous work has established a stochastic model for a CMOS circuit that describes the dynamics of the elementary steps and accounts for the thermodynamic cost [19–21], validated by agreement with experiments [22]. The master-equation model was numerically solved, giving access to both error and dissipation rates [18, 20]. Extending that approach to larger circuits is tempting to do via coarser descriptions—replacing discrete electron hops with continuous voltage noise—but doing so severs the thermodynamically consistent link between circuit energetics and thermal fluctuations that local detailed balance enforces at each elementary step. One is therefore caught between two undesirable options: retain microscopic discreteness and face a state space too large for conventional methods, or adopt a tractable coarse-grained description and sacrifice thermodynamic fidelity. Tensor network methods resolve this tension by efficiently representing the high-dimensional probability distribution without explicitly enumerating the exponentially large state space.

Here, we introduce tensor network (TN) methods [23–27] combined with a judicious basis set expansion to stochastic electronic circuits, numerically solving for the steady-state thermodynamics (dissipation rate) and the relaxation timescales (error rate) for bistable coupled circuits. The main results are twofold. First, we demonstrate that a higher accuracy can be achieved either by

---

\* [emanuele.penocchio@northwestern.edu](mailto:emanuele.penocchio@northwestern.edu)

† [todd.gingrich@northwestern.edu](mailto:todd.gingrich@northwestern.edu)

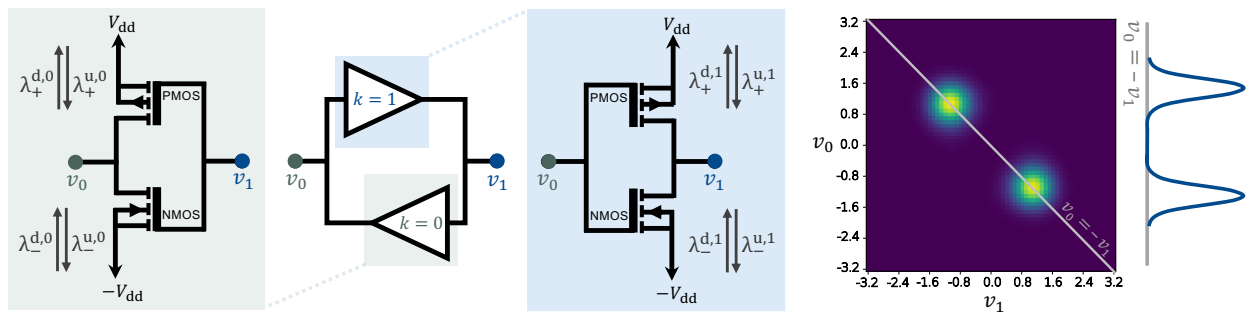


FIG. 1. The minimal instantiation of a bit with CMOS technology is a single unit with two nodes at voltages  $v_0$  and  $v_1$ . These nodes are coupled by two NOT gates, each consisting of an n-type (-) and p-type (+) transistor. In all four transistors, electrons hop in both directions between ideal thermodynamic reservoirs ( $-V_{dd}$  and  $V_{dd}$ ) and the fluctuating voltage nodes. Rates for those hops,  $\lambda$ , depend on  $\mathbf{v}$ , with three indices indicating the NOT gate, the n/p transistor, and the direction of the hop. The coupled nodes yield a bistable steady state (right), with each peak corresponding to a metastable bit-state.

increasing the supply voltage or by daisy chaining together units, and that the former strategy results in less dissipation while the latter can be useful for low-voltage computing. Second, we establish tensor network methods to significantly advance numerical analysis of stochastic circuit models capable of faithfully resolving both rare events and thermodynamics, by preserving the discrete thermal noise from which thermodynamic consistency emerges even for systems exceeding  $10^{14}$  microstates. Although our focus in this work is on circuits built by combining identical units in series, the methodology naturally extends to situations in which the units are not identical (such as due to fabrication variability or degradation [28–31]), or are combined in more complicated architectures [32, 33]. Finally, we propose that our framework be applied to CMOS phenomena where thermal noise is a feature, rather than a bug, such as in its application to thermodynamic computing [22, 34, 35].

*Dynamics and Thermodynamics of a Single CMOS Unit.* A single CMOS unit is typically built from two NOT gates, each consisting of an n-type and p-type metal oxide semiconductor field effect transistor (MOSFET) through which electrons can hop bidirectionally between a source at voltage  $-V_{dd}$  and a drain at voltage  $V_{dd}$ . The permitted electron hops associated with each transistor in the single unit are shown in Figure 1. The unit’s state is given by the vector  $\mathbf{v} = (v_0, v_1)$ , with voltages  $v_0$  and  $v_1$  measured at nodes on opposite sides of the unit. The hop rates depend on the state of the circuit through  $\mathbf{v}$ , the characteristics of the device through a threshold voltage  $V_{th}$  and subthreshold slope factor  $n$ , and the temperature  $T$  through a thermal voltage  $V_T = k_B T/e$ , where  $k_B$  is Boltzmann constant and  $e$  the charge of an electron.

With two orientations of NOT gates and two transistors per gate, there are four junctions across which electrons hop. Each elementary hop also includes a direction, either “uphill” or “downhill”, referring to the direction of the mean flow of electrons (from source to drain). The hops are frequently modeled as Poissonian transitions which alter the voltage at one of the two nodes by

a discrete amount  $v_e = e/C$ , where  $C$  is the capacitance of the transistor. We write the rate of an uphill hop as

$$\lambda_{\pm}^{u,k}(\mathbf{v}) = \exp\left(\frac{V_{dd} - V_{th} \mp \delta_{k,1}v_0 \mp \delta_{k,0}v_1}{nV_T}\right), \quad (1)$$

where the  $\pm$  subscript differentiates between hops in the n-type (-) and p-type (+) MOSFETs and the  $k$  index selects for the bottom NOT gate ( $k = 0$ , shaded gray) or the top ( $k = 1$ , shaded blue) in Fig. 1. Hops in NOT gate  $k$  cause  $v_k$  to change while the voltage of the other node stays fixed. The Kronecker  $\delta$  functions of Eq. (1) imply that uphill steps that change each node’s voltage occur with a rate that depends only on the value of the other node’s voltage. The rates of downhill hops take a similar form, but depend on both  $v_0$  and  $v_1$ :

$$\lambda_{\pm}^{d,k}(\mathbf{v}) = \lambda_{\pm}^{u,k}(\mathbf{v}) \exp\left(\frac{-V_{dd} - \frac{1}{2}v_e \pm \delta_{k,0}v_0 \pm \delta_{k,1}v_1}{V_T}\right). \quad (2)$$

For every electron that hops downhill at a p-type MOSFET or uphill at an n-type, the altered voltage ( $v_0$  or  $v_1$ ) goes down by the discrete step  $v_e$ . Similarly, jumps in the opposite direction increase voltages by that same  $v_e$ .

The discrete hops cause the voltage to fluctuate according to a master equation

$$\frac{\partial \vec{P}}{\partial t} = \mathbb{W} \vec{P}, \quad (3)$$

where  $\vec{P}$  is a vector of probabilities of each microstate, specified by the voltage values at both nodes 0 and 1. Because each of these voltages can take a discrete number of possible values, the operator  $\mathbb{W}$  is the usual continuous-time transition rate matrix with off-diagonal elements expressed in terms of  $\lambda_{\pm}^{u,k}$  and  $\lambda_{\pm}^{d,k}$  and diagonal elements ensuring the conservation of probability. The stochastic dynamics samples values of  $v_0$  and  $v_1$  from the non-equilibrium steady-state distribution  $P_{ss}(\mathbf{v})$  that solves  $\mathbb{W} \vec{P} = 0$ . The symmetry of the gates that make up the CMOS circuit furthermore ensures a symmetry in the

probabilities,  $P_{\text{ss}}(\mathbf{v}) = P_{\text{ss}}(-\mathbf{v})$ , that yields a bistability, shown in Fig. 1. A voltage drop across the circuit is equally likely to be positive as negative, allowing the CMOS circuit to be thought of as a physical instantiation of a logical bit. The first excited state eigenvalue and eigenvector of  $\mathbb{W}$  give the timescale and mode of relaxation between the two states of the bit [27, 36].

It is also interesting to consider flows of energy that accompany the stochastic dynamics. Elementary uphill and downhill hops move electrons between ideal thermodynamic reservoirs held at particular voltages and temperature  $T$ . Microscopic reversibility of the elementary steps gives the local detailed balance condition:

$$-k_{\text{B}}T \log \frac{\lambda_{\pm}^{\text{u},k}(\mathbf{v})}{\lambda_{\pm}^{\text{d},k}(\mathbf{v} \pm v_e(\delta_{k,0}, \delta_{k,1}))} = \delta Q_{\pm}(v_k), \quad (4)$$

where

$$\delta Q_{\pm}(v_k) = e \left( -V_{\text{dd}} + \frac{1}{2}v_e \pm v_k \right) \quad (5)$$

is the energy flow from bath to system when moving a single electron between node  $k$  and a thermodynamic reservoir (source/drain) in the uphill  $v_k \rightarrow v_k \pm v_e$  direction [19]. This local detailed balance condition is what ties the circuit energetics directly to the thermal fluctuations, and it is the property we must preserve when extending to larger circuits. In the steady state, the net rate of these uphill steps is the particle current

$$j_{\pm}^k(\mathbf{v}) = \lambda_{\pm}^{\text{u},k}(\mathbf{v})P_{\text{ss}}(\mathbf{v}) - \lambda_{\pm}^{\text{d},k}(\mathbf{v} \pm v_e(\delta_{k,0}, \delta_{k,1}))P_{\text{ss}}(\mathbf{v} \pm v_e(\delta_{k,0}, \delta_{k,1})), \quad (6)$$

where the  $\pm$  again distinguishes between the current through n- and p-type transistors and  $k$  selects the NOT gate's orientation. The average dissipation rate for the entire CMOS circuit sums over contributions from each transistor for each microstate  $\mathbf{v}$ :

$$\dot{Q} = \sum_{v_0, v_1} \sum_{\alpha=\pm} \sum_k \delta Q_{\alpha}(v_k) j_{\alpha}^k(\mathbf{v}). \quad (7)$$

*Coupling CMOS Units to Make a Collective Bit.* Having established the dynamics and thermodynamics of a single CMOS unit, we now build a larger circuit from  $L$  units, connected in series. The state  $\mathbf{v}$  of the CMOS chain is characterized by a higher dimensional vector whose components  $v_i$  indicate the voltage of each node between the units. The rate of elementary hops across a MOSFET in unit  $i = 0, 1, \dots, L-1$  is again given by expressions of the form given in Eqs. 1 and 2 except that elementary hops within unit  $i$  now depend on  $v_i$  and  $v_{i+1}$ . As before, each discrete hop changes one of these voltages by  $v_e$ .

Provided that the supply voltage is large enough to support bistability ( $V_{\text{dd}} \geq V_T \ln 2$  for  $n = 1$ ), voltages at neighboring nodes become strongly anti-correlated with each other.  $P_{\text{ss}}(\mathbf{v})$  for a chain with an odd number of  $L$

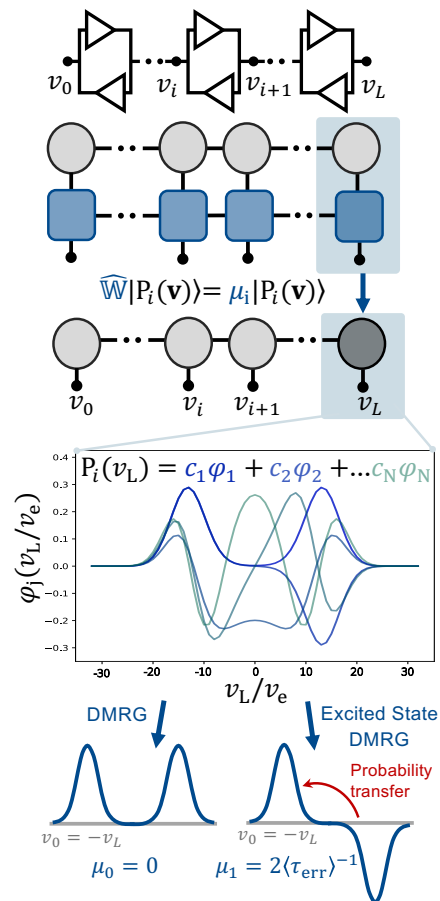


FIG. 2. The rate operator, Eq. (10), can be compressed into a matrix product operator (MPO), shown in blue. Right eigenvectors of the single-CMOS-unit problem are used as basis vectors  $\phi_i$ , and DMRG is used to find controllable approximations for the top two right eigenvectors of the  $L$ -unit problem.

units is therefore dominated by one of two symmetrically equivalent macrostates, each with large voltages of alternating sign. The transition from one macrostate to the other is a rare event that requires all nodes to flip their voltage, so the CMOS chain acts as a single collective bit. The characteristic timescale for that bit flip,  $\langle \tau_{\text{err}} \rangle$ , depends on the number of units in the chain, with longer chains suppressing the rate of spontaneous bit flips. An alternative strategy to increase  $\langle \tau_{\text{err}} \rangle$  is to increase the supply voltage  $V_{\text{dd}}$ . Both strategies to enhance bit stability come with a dissipative cost.

To analyze tradeoffs, we need a numerical strategy to compute both  $\langle \tau_{\text{err}} \rangle$  and  $\dot{Q}$  for CMOS chains. In principle, the calculations are straightforward. The top right eigenvector of  $\mathbb{W}$  is  $P_{\text{ss}}(\mathbf{v})$ , from which particle currents and dissipation are computed as in Eqs. 6 and 7. The next eigenvector captures the slowest relaxation mode, with associated eigenvalue  $\mu_1$  giving the flipping timescale through:  $\langle \tau_{\text{err}} \rangle = \frac{2}{\mu_1}$  [36]. In practice, calculations of the principal eigenvector and the spectral gap are nontrivial because  $L$ -unit chains introduce a many-

body problem. Consequently, we adopt a TN approach to obtain numerically exact results with enormous state spaces ( $3 \times 10^{14}$  microstates in the  $L = 7$ ,  $V_{dd} = 1.4$  calculation).

To employ this approach we first must write the rate operator in a second-quantized form. Recognize that each elementary electron hop induces a discrete jump of the voltage at a single node, so we introduce the raising and lowering operators

$$\hat{x}_i^\pm |\mathbf{v}\rangle = |v_1, \dots, v_i \pm v_e, \dots, v_N\rangle, \quad (8)$$

with  $|\mathbf{v}\rangle$  being a Fock vector for microstate  $\mathbf{v}$ . Each hop in voltage can be induced by electron hopping events at multiple different transistors, and the rates for each of those hops depend on the voltages. To compactly compute rates of each event, we introduce, for each CMOS unit  $i$ , diagonal operators  $\hat{t}_{\pm,i}^{u/d}$  and  $\hat{b}_{\pm,i}^{u/d}$  giving the hop-

ping rates in the top and bottom NOT gates, respectively. Mirroring Eqs. (1) and (2),

$$\begin{aligned} \hat{b}_{\pm,i}^u |\mathbf{v}\rangle &= \exp\left(\frac{V_{dd} - V_{th} \mp v_{i+1}}{nV_T}\right) |\mathbf{v}\rangle \\ \hat{b}_{\pm,i}^d |\mathbf{v}\rangle &= \hat{b}_{\pm,i}^u \exp\left(\frac{-V_{dd} - \frac{1}{2}v_e \pm v_i}{V_T}\right) |\mathbf{v}\rangle. \end{aligned} \quad (9)$$

Equivalent expressions for  $\hat{t}_{\pm,i}^u$  and  $\hat{t}_{\pm,i}^d$  simply change  $b$ 's to  $t$ 's and exchange the positions of  $v_i$  and  $v_{i+1}$  in Eq. (9) since the top NOT gate is oriented in the opposite direction from the bottom. The rate operator includes contributions from uphill and downhill hops through all 4 transistors and sums over all CMOS units:

---


$$\hat{\mathbb{W}} = \sum_{i=0}^{L-1} \left[ (\hat{t}_{+,i}^u + \hat{t}_{-,i}^d) (\hat{x}_{i+1}^+ - \mathbb{I}_{i+1}) + (\hat{t}_{+,i}^d + \hat{t}_{-,i}^u) (\hat{x}_{i+1}^- - \mathbb{I}_{i+1}) + (\hat{b}_{+,i}^u + \hat{b}_{-,i}^d) (\hat{x}_i^+ - \mathbb{I}_i) + (\hat{b}_{+,i}^d + \hat{b}_{-,i}^u) (\hat{x}_i^- - \mathbb{I}_i) \right]. \quad (10)$$

Here, it is understood that  $\hat{x}_i^\pm = \mathbb{I}_0 \otimes \dots \otimes x_i^\pm \otimes \dots \otimes \mathbb{I}_L$ , with implicit identity operators. The additional explicit identity operators of Eq. (10) generate the negative diagonal elements that ensure probability conservation. This representation in terms of raising and lowering operators lends itself to an efficient compression in terms of a matrix product operator (MPO), which we constructed using the AutoMPO function of the ITensor.jl tensor networks toolkit [37]. The result is an MPO with bond dimension 6 connecting together the  $L + 1$  sites, reflecting the fact that each elementary hop couples only nearest-neighbor sites. The state of each site corresponds to the voltage of a node, voltages which can only be discrete multiples of  $v_e$ . In practice, the CMOS architecture prevents the magnitudes of the voltages from growing without bound, so it is reasonable to truncate the allowable voltage values at some large positive and negative threshold. For the calculations we present in Fig. 3, it was sufficient to allow voltages to run from  $-32v_e$  to  $32v_e$ , meaning the MPO has a physical dimension  $D = 65$ .

The MPO requires a very small bond dimension because it only needs to capture the correlations between neighboring sites in an infinitesimal time propagation. In other words, the MPO only needs to capture how one elementary hop impacts multiple different sites. By contrast, we also need a TN approximation to the probability distribution  $P_{ss}(\mathbf{v})$ , and that distribution can include strong correlations between distant sites which have formed as a consequence of many elementary hops. Our interest is in CMOS chains that are relatively short ( $L \leq 7$ ), and we find we can capture those correlations with a matrix product state (MPS) with modest

( $\leq 100$ ) bond dimension. We perform sweeps of single-site DMRG with a local Arnoldi solver to converge to an MPS approximation for  $|P_{ss}\rangle$ , the top right eigenvector associated with the zero eigenvalue. That principal eigenvector is stationary under the DMRG sweeps even though  $\hat{\mathbb{W}}$  is non-hermitian [27]. We furthermore apply the penalty method with single-site DMRG sweeps to compute the spectral gap  $\mu_1$  and the associated eigenvector  $|P_{relax}\rangle$ , which characterizes the slowest relaxation to the steady state [38].

Both DMRG calculations are less expensive if the physical dimension can be compressed. We find we are able to roughly halve the physical dimension if we work with a judicious basis set expansion. As illustrated in Fig. 2, we solve for the right eigenvectors of  $\hat{\mathbb{W}}$  when  $L = 1$  with an exact diagonalization. These single-CMOS calculations both validate the truncation  $|v_i| \leq 32v_e$  but also allow us to perform the MPS calculation in terms of a modest number of coefficients for the most important basis functions. In practice, we initialize the MPS to give a uniform distribution over all voltage states and perform DMRG sweeps with a small maximal bond dimension and with few retained basis functions. As the MPS converges, both cutoffs are increased.

Having computed the MPS for the steady-state distribution,  $Q$  is straightforward to extract. We turn Eq. (5) into the diagonal operator

$$\hat{\delta}Q_{\pm,i} |\mathbf{v}\rangle = e(-V_{dd} + \frac{v_e}{2} \pm v_i) |\mathbf{v}\rangle, \quad (11)$$

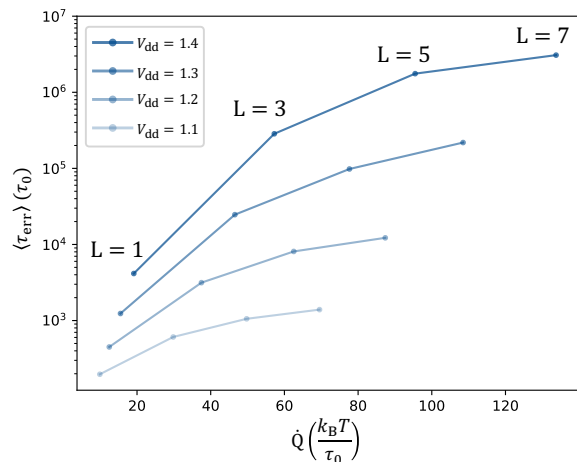


FIG. 3. Reliability vs. dissipation tradeoff for CMOS chains. The mean time between bit-flip errors  $\langle \tau_{\text{err}} \rangle$  (left) increases exponentially with bias voltage  $V_{\text{dd}}$  but subexponentially with chain length  $L$ . Steady-state dissipation  $\dot{Q}$  (right) scales linearly with both  $V_{\text{dd}}$  and  $L$ . Consequently, for any fixed dissipation budget (horizontal line), maximum reliability is achieved with minimum  $L$  and maximum  $V_{\text{dd}}$ . Both quantities normalized by the characteristic circuit timescale  $\tau_0 = \frac{e}{I_0} e^{V_{\text{th}}/(nV_T)}$ , where  $I_0$  is the specific current of the transistor.

to get

$$\dot{Q} = 2 \sum_{i=0}^{L-1} \sum_{\alpha=\pm} \langle \mathbf{1} | \delta \hat{Q}_{\alpha, i+1} (\hat{t}_{\alpha, i}^{\text{u}} - \hat{t}_{\alpha, i}^{\text{d}} \hat{x}_{i+1}^{-\alpha}) | P_{\text{ss}} \rangle, \quad (12)$$

where  $\langle \mathbf{1} |$  is the vector of all ones. For compactness, we have double counted the dissipation through the top NOT gates since  $|P_{\text{ss}}\rangle$  is symmetric.

*Dissipation-Reliability Trade-off.* We found  $|P_{\text{ss}}\rangle$  and  $|P_{\text{relax}}\rangle$  with DMRG to compute  $\langle \tau_{\text{err}} \rangle$  and  $\dot{Q}$  for CMOS chains with  $L = 1, 3, 5, 7$  and with  $V_{\text{dd}}$  ranging from 1.1V through 1.4V. There are two distinct ways to make robust bits last longer, increasing  $V_{\text{dd}}$  or  $L$ . The dependence with  $V_{\text{dd}}$  is simplest. A barrier between metastable states grows proportionally to  $V_{\text{dd}}^2$ , and an Arrhenius law anticipates that  $\ln \langle \tau_{\text{err}} \rangle$  would grow in proportion to  $V_{\text{dd}}^2$

[18], as we find in our calculations. In related work looking at metastable transitions of reaction-diffusion systems, we similarly observed that log transition rates grew in proportion to a barrier height, but the scaling with  $L$  was different. For the reaction-diffusion calculations, the log transition rates grew in proportion to the number of units in a 1D chain [26]. In contrast, for the CMOS chains, we see that  $\ln \langle \tau_{\text{err}} \rangle$  grows *sublinearly* with  $L$ , reflecting a nontrivial collective effect of the inter-unit correlations. The consequence is that increasing  $V_{\text{dd}}$  is in a sense a more effective way to extend  $\langle \tau_{\text{err}} \rangle$  than increasing  $L$ .

The advantage of increasing  $V_{\text{dd}}$  is particularly clear if the cost is the dissipation. While the error time  $\langle \tau_{\text{err}} \rangle$  is determined by rare events,  $\dot{Q}$  is the typical steady-state dissipation, which is dominated by the dissipation through all transistors at the typical voltage. The number of dissipating transistors grows linearly with  $L$ , and the typical voltage grows linearly with  $V_{\text{dd}}$ . Consequently, the dissipative cost  $\dot{Q}$  grows linearly with both  $L$  and  $V_{\text{dd}}$ . For a fixed dissipation budget, Fig. 3 thus shows that the most robust bit is that with the smallest  $L$ . However, it is not necessarily the case that dissipation minimization is always the goal. Faced with the constraint to build a CMOS bit with small errors and with a maximal  $V_{\text{dd}}$ , the results show that it can be efficacious to grow the chain.

There are several directions for interesting future work. Though here applied for chains with identical CMOS devices, the TN methods extend naturally to systems with device variability [28–31] and to more complicated architectures [32, 33]. Developments in methods for looped tensor networks [39] could also be used to evaluate bit changes in rings or with periodic boundary conditions. We can also apply these methods to determine the proximity of more complex CMOS architectures to fundamental limits on charging speed and computational modularity [10, 20, 33, 40, 41] and assess other stochastic electronic technologies [11–13, 42, 43], including those developed for thermodynamic computing algorithms [9, 22, 34, 35, 44–48]. Even more ambitiously, similar calculations could illuminate robustness-dissipation tradeoffs in biochemical reaction networks [27, 49–51], perhaps leveraging applications of modular circuit theory to chemical reaction networks [52, 53].

- 
- [1] A. Wang, B. H. Calhoun, and A. P. Chandrakasan, *Sub-threshold Design for Ultra Low-Power Systems* (Springer, 2006).
- [2] K. Natori and N. Sano, Scaling limit of digital circuits due to thermal noise, *J. Appl. Phys.* **83**, 5019 (1998).
- [3] E. Rezaei, M. Donato, W. R. Patterson, A. Zaslavsky, and R. I. Bahar, Fundamental thermal limits on data retention in low-voltage CMOS latches and SRAM, *IEEE Trans. Device Mater. Reliab.* **20**, 488 (2020).
- [4] R. Landauer, Irreversibility and heat generation in the

- computing process, *IBM J. Res. Dev.* **5**, 183 (1961).
- [5] A. Bryant, J. Brown, P. Cottrell, M. Ketchen, J. Ellis-Monaghan, and E. J. Nowak, Low-power CMOS at  $V_{\text{dd}} = 4kT/q$ , in *Device Research Conference* (2001) pp. 22–23.
- [6] D. Bol, R. B. Ambroise, D. Flandre, and J.-D. Legat, Interests and limitations of technology scaling for sub-threshold logic, *IEEE Trans. Very Large Scale Integr. Syst.* **17**, 1508 (2009).
- [7] S. Hanson, M. Seok, D. Sylvester, and D. Blaauw, Nanometer device scaling in subthreshold logic and

- SRAM, *IEEE Trans. Electron Devices* **55**, 175 (2008).
- [8] K. Kim and V. D. Agrawal, Minimum energy CMOS design with dual subthreshold supply and multiple logic-level gates, in *12th Int. Symp. Quality Electronic Design* (2011) pp. 1–6.
- [9] M. Aifer, D. Melanson, K. Donatella, G. Crooks, T. Ahle, and P. J. Coles, [Error mitigation for thermodynamic computing](#) (2024), [arXiv:2401.16231 \[cs.ET\]](#).
- [10] P. M. Riechers, A. B. Boyd, G. W. Wimsatt, and J. P. Crutchfield, Balancing error and dissipation in computing, *Phys. Rev. Res.* **2**, 033524 (2020).
- [11] J. Rivnay, P. Leleux, M. Sessolo, D. Khodagholy, T. Hervé, M. Fiocchi, and G. G. Malliaras, Organic electrochemical transistors with maximum transconductance at zero gate bias, *Adv. Mater.* **25**, 7010 (2013).
- [12] H. Sun, M. Vagin, S. Wang, X. Crispin, R. Forchheimer, M. Berggren, and S. Fabiano, Complementary logic circuits based on high-performance n-type organic electrochemical transistors, *Adv. Mater.* **30**, 1704916 (2018).
- [13] Y. Jia, Q. Jiang, H. Sun, P. Liu, D. Hu, Y. Pei, W. Liu, X. Crispin, S. Fabiano, Y. Ma, and Y. Cao, Wearable thermoelectric materials and devices for self-powered electronic systems, *Adv. Mater.* **33**, 2102990 (2021).
- [14] L. Weiss and W. Mathis, A thermodynamical approach to noise in non-linear networks, *Int. J. Circuit Theory Appl.* **26**, 147 (1998).
- [15] R. Sarpeshkar, T. Delbruck, and C. A. Mead, White noise in MOS transistors and resistors, *IEEE Circuits Devices Mag.* **9**, 23 (1993).
- [16] J. L. Wyatt and G. J. Coram, Nonlinear device noise models: Satisfying the thermodynamic requirements, *IEEE Trans. Electron Devices* **46**, 184 (1999).
- [17] P. Hänggi and P. Jung, Bistability in active circuits: Application of a novel Fokker-Planck approach, *IBM J. Res. Dev.* **32**, 119 (1988).
- [18] N. Freitas, K. Proesmans, and M. Esposito, Reliability and entropy production in nonequilibrium electronic memories, *Phys. Rev. E* **105**, 034107 (2022).
- [19] N. Freitas, J. C. Delvenne, and M. Esposito, Stochastic thermodynamics of nonlinear electronic circuits: A realistic framework for computing around  $kT$ , *Phys. Rev. X* **11**, 031064 (2021).
- [20] C. Y. Gao and D. T. Limmer, Principles of low dissipation computing from a stochastic circuit model, *Phys. Rev. Res.* **3**, 033169 (2021).
- [21] J. Gu and P. Gaspard, Microreversibility, fluctuations, and nonlinear transport in transistors, *Phys. Rev. E* **99**, 012137 (2019).
- [22] N. Freitas, G. Massarelli, J. Rothschild, D. Keane, E. Dawe, S. Hwang, A. Garlapati, and T. McCourt, Taming nonequilibrium thermal fluctuations in subthreshold CMOS circuits, *Phys. Rev. Appl.* (2026).
- [23] G. Evenbly and G. Vidal, Tensor network states and geometry, *J. Stat. Phys.* **145**, 891 (2011).
- [24] V. Kazeev, M. Khammash, M. Nip, and C. Schwab, Direct solution of the chemical master equation using quantized tensor trains, *PLOS Comput. Biol.* **10**, e1003359 (2014).
- [25] H. D. Vo and R. B. Sidje, An adaptive solution to the chemical master equation using tensors, *J. Chem. Phys.* **147**, 044102 (2017).
- [26] S. B. Nicholson and T. R. Gingrich, Quantifying rare events in stochastic reaction-diffusion dynamics using tensor networks, *Phys. Rev. X* **13**, 041006 (2023).
- [27] J. P. Zima, S. B. Nicholson, and T. R. Gingrich, Chemical master equation parameter exploration using DMRG, *J. Chem. Phys.* **163**, 054118 (2025).
- [28] A. Asenov, A. R. Brown, J. H. Davies, S. Kaya, and G. Slavcheva, Simulation of intrinsic parameter fluctuations in decananometer and nanometer-scale MOSFETs, *IEEE Trans. Electron Devices* **50**, 1837 (2003).
- [29] S. Mukhopadhyay, H. Mahmoodi, and K. Roy, Modeling of failure probability and statistical design of SRAM array for yield enhancement in nanoscaled CMOS, *IEEE Trans. Comput.-Aided Des. Integr. Circuits Syst.* **24**, 1859 (2005).
- [30] H. Mahmoodi, S. Mukhopadhyay, and K. Roy, Estimation of delay variations due to random-dopant fluctuations in nanoscale CMOS circuits, *IEEE J. Solid-State Circuits* **40**, 1787 (2005).
- [31] M. Maghsoudloo, On the prevention of coherence-induced static noise margin degradation of SRAM cells, in *5th CPSSI Int. Symp. Cyber-Phys. Syst.* (2024).
- [32] K. Ueda, Z. Rikuhashi, K. Hayashi, and H. Hikawa, Low-power wiring method in CMOS logics circuits by segmentation coding and pseudo majority voting, *IEEE Int. Symp. Circuits Syst.* , 590 (2014).
- [33] D. H. Wolpert and A. Kolchinsky, Thermodynamics of computing with circuits, *New J. Phys.* **22**, 063047 (2020).
- [34] S. Chowdhury, A. Grimaldi, N. A. Aadit, S. Niazi, M. Mohseni, S. Kanai, H. Ohno, S. Fukami, L. Theogarajan, G. Finocchio, S. Datta, and K. Y. Camsari, A full-stack view of probabilistic computing with p-bits: Devices, architectures, and algorithms, *IEEE J. Explor. Solid-State Comput. Devices Circuits* **9**, 1 (2023).
- [35] T. Conte, E. DeBenedictis, N. Ganesh, T. Hylton, J. P. Strachan, R. S. Williams, A. Alemi, L. Altenberg, G. Crooks, J. Crutchfield, L. del Rio, J. Deutsch, M. DeWeese, K. Douglas, M. Esposito, M. Frank, R. Fry, P. Harsha, M. Hill, C. Kello, J. Krichmar, S. Kumar, S.-C. Liu, S. Lloyd, M. Marsili, I. Nemenman, A. Nugent, N. Packard, D. Randall, P. Sadowski, N. Santhanam, R. Shaw, A. Stieg, E. Stopnitzky, C. Teuscher, C. Watkins, D. Wolpert, J. Yang, and Y. Yufik, [Thermodynamic computing](#) (2019), [arXiv:1911.01968 \[cs.CY\]](#).
- [36] B. Roux, Transition rate theory, spectral analysis, and reactive paths, *J. Chem. Phys.* **156**, 134111 (2022).
- [37] M. Fishman, S. R. White, and E. M. Stoudenmire, The ITensor software library for tensor network calculations, *SciPost Phys. Codebases* , 4 (2022).
- [38] E. M. Stoudenmire and S. R. White, Studying two-dimensional systems with the density matrix renormalization group, *Annu. Rev. Condens. Matter Phys.* **3**, 111 (2012).
- [39] S. Midha and Y. F. Zhang, [Beyond belief propagation: Cluster-corrected tensor network contraction with exponential convergence](#) (2025), [arXiv:2510.02290 \[quant-ph\]](#).
- [40] P. Helms, S. W. Chen, and D. T. Limmer, Stochastic thermodynamic bounds on logical circuit operation, *Phys. Rev. E* **111**, 034110 (2025).
- [41] A. B. Boyd, D. Mandal, and J. P. Crutchfield, Thermodynamics of modularity: Structural costs beyond the Landauer bound, *Phys. Rev. X* **8**, 031036 (2018).
- [42] V. J. Dowling, V. A. Slipko, and Y. V. Pershin, Probabilistic memristive networks: Application of a master equation to networks of binary ReRAM cells, *Chaos Soliton. Fract.* **142**, 110530 (2021).
- [43] V. A. Slipko and Y. V. Pershin, Theory of heterogeneous

- circuits with stochastic memristive devices, *IEEE Trans. Circuits Syst. II* **69**, 214 (2022).
- [44] D. Melanson, M. Abu Khater, M. Aifer, K. Donatella, M. H. Gordon, T. Ahle, G. Crooks, A. J. Martinez, F. Sbahi, and P. J. Coles, Thermodynamic computing system for AI applications, *Nat. Commun.* **16**, 3757 (2025).
- [45] S. Whitelam and C. Casert, Nonlinear thermodynamic computing out of equilibrium, *Nat. Commun.* **17**, 1189 (2026).
- [46] J. Kim, J.-K. Han, H.-Y. Maeng, J. Han, J. W. Jeon, Y. H. Jang, K. S. Woo, Y.-K. Choi, and C. S. Hwang, Fully CMOS-based p-bits with a bistable resistor for probabilistic computing, *Adv. Funct. Mater.* **34**, 2307935 (2024).
- [47] P. J. Coles, C. Szczepanski, D. Melanson, K. Donatella, A. J. Martinez, and F. Sbahi, Thermodynamic AI and the fluctuation frontier, in *IEEE Int. Conf. Rebooting Computing (ICRC)* (2023) pp. 1–10.
- [48] M. Aifer, K. Donatella, M. H. Gordon, S. Duffield, T. Ahle, D. Simpson, G. Crooks, and P. J. Coles, Thermodynamic linear algebra, *npj Unconv. Comput.* **1**, 13 (2024).
- [49] G. Tkačik and P. R. ten Wolde, Information processing in biochemical networks, *Annu. Rev. Biophys.* **54**, 249 (2025).
- [50] T. E. Ouldridge, C. C. Govern, and P. R. ten Wolde, Thermodynamics of computational copying in biochemical systems, *Phys. Rev. X* **7**, 021004 (2017).
- [51] S. B. Nicholson and L. P. García-Pintos, *Thermodynamics of large-scale chemical reaction networks* (2025), [arXiv:2512.19616 \[cond-mat.stat-mech\]](https://arxiv.org/abs/2512.19616).
- [52] F. Avanzini, N. Freitas, and M. Esposito, Circuit theory for chemical reaction networks, *Phys. Rev. X* **13**, 021041 (2023).
- [53] P. Raux, C. Goupil, and G. Verley, Thermodynamic circuits: Modeling chemical reaction networks with nonequilibrium conductance matrices, *Phys. Rev. E* **112**, 034112 (2025).